International Journal of
INTELLIGENT SYSTEMS AND APPLICATIONS IN ENGINEERING
ISSN:2147-6799 www.ijisae.org Original Research Paper

Mapbi3 Perovskite Solar Structure Experimental Optimization: Control of Deposition of Spinning Speed (Comparative Study of Optical and Structural Proprieties)

Aicha Aziza Ayad[1], Abdelkrim Naas[1], Ahmed Gueddim[1], Mohamed Elbar*[2]

Received: 08/01/2025 **Accepted:** 25/02/2025 **Published:** 15/03/2025

Abstract: The present paper deals with the stability of halide hybrid perovskite MAPbI3 (CH3NH3PbI3) thin films by an experimental optimization by increasing the Dimethyl sulfoxide (DMSO) solvent ratio (compared to literature) in perovskite solution and the study of deposition spinning speed effect on the structural and optical properties. The samples is deposited by a spin coater in one step with 400, 1500 and 3000 rpm spinning speed. Structural and optical properties of the elaborated samples were studied using X-ray diffraction and UV-Visible spectroscopy. The main results show that compared with other works the DMSO solvent ration raise has a positive effect in the perovskite proprieties, in other hand, the best proprieties of perovskite need an optimal speed deposition; the very high or low speed has a negative effect.

Keywords: *Perovskite solar cells, MAPbI3, spinning speed.*

1. Introduction

The third generation of solar cells saw the appearance of perovskite cells (PSCs). The perovskite material stands as the intrinsic layer in the PIN structure of the solar cell. The halide hybrid perovskite consists of an organic-inorganic compound that adopts the general chemical formula AMX3, in which 'A' organic cation, 'M' are inorganic cation and 'X' is an anion [1]. Our perovskite MAPbI3 is a semiconductor has a direct gap around 1.40 to 1.64ev [2-8], has a simple elaboration with cheap base materials [7] and possesses a high absorbance [8].Our structure loss its organic part during or after elaboration by the light, humidity, heat or air ,these factors causes a great degradation appears as a rise of inorganic element percentage (PbI2) reflecting its instability [2,9-11].Previous improvements made by researchers to our structure was divided on three sections (impact of impurities inclusion, structure cations changing effect and the elaboration optimization) [12-21].

The improving of perovskite elaboration by reaching the optimal conditions can reduce the problem of its instability, this is what we saw in our previous study (the substrate type impact) [22].In this paper we chose the study of deposition speed effect on the structural and optical properties with an increasing of Dimethyl sulfoxide (DMSO) solvent ration (compared to literature) on the perovskite synthesis which previously unused for MAPbI3 elaboration.

1 Department of Materials Science and Informatics Laboratory, University of Djelfa 17000, Djelfa, Algeria a.ayad@univ-djelfa.dz

2 Applied Automation and Industrial Diagnostics Laboratory (LAADI), Faculty of Science and Technology, Ziane Achour University of Djelfa, Djelfa 17000, Algeria

** Corresponding Author Email: m.elbar@univ-djelfa.dz*

2. Experimental Section

2.1. Samples elaboration

We used two powders CH3NH3I and PbI2 dissolved in N, N-dimethylformamide (DMF) solvents and Dimethyl sulfoxide (DMSO) with a ration (1:4). The resulting solution was stirred at 60°C overnight. The films were prepared by spin coating on cleaned glass substrates. We used centrifugation speed 400, 1500 and 3000 rpm for 20 s. Subsequently, the freshly deposited films were annealed at 70 °C for 15 min. Regarding the XRD analysis we used a Xpert-Pro MPD of Philips diffractometer system with Cu-Kα radiation 1.54060 Å, for UV-visible we used the Shimadzu UV-1800 UV-Vis spectrophotometer with wavelength range 300 to 700 nm, the results tracer by logiciel 'Origine6'.

2.2. Samples elaboration

The MAPI3 gap energy was obtained from Tauc law (Eq.1) [7], where α the absorption coefficient, h is the Plank constant, μ is the frequency of light, A constant. The absorption coefficient α was obtained from (Eq.2), where d the layer thickness of the thin film and T is it a transmittance. The layer thickness d was obtained from the (Eq.3) [23], where M is the mass of the thin film, ρ is MAPbI3 materiel density
(4.15gr/cm3) and s is the surface of sample. The mass M obtained from (Eq.4), where Mi is the masse of substrate and Mf is the masse of sample after deposition of the film. The phases percentage were calculated from (Eq.5) where A is the PbI2 integration peaks, B is CH3NH3PbI3 integration peaks and C is the diffractogram integration [24]. Preferential orientation R I(hkl) was calculated from (Eq.6) [25], where Ihkl present the intensity of peak. The grain size D was calculated from (Eq.7), where K is the Scherrer constant (0.9), λ is wave length of the X-ray beam used (1.54060 Å), β is the Full width at half maximum (FWHM)

of the peak and θ is the Bragg angle. The dislocation density σ was calculated from (Eq.8) [26].

$$\alpha h\mu = A\sqrt{h\mu - E_g} \quad (1)$$

$$\alpha = \frac{1}{d}\ln\frac{100}{T} \quad (2)$$

$$d = \frac{M}{\rho s} \quad (3)$$

$$M = (M_f - M_i) \quad (4)$$

$$\begin{cases} P_{Pb2}\,(\%) = \frac{A\times 100(\%)}{C} \\ \text{et} \\ P_{CH3NH3PbI3}\,(\%) = \frac{B\times 100(\%)}{C} \end{cases} \quad (5)$$

$$R_{I(hkl)} = \frac{I_{hkl}}{\sum I_{(hkl)}} \quad (6)$$

$$D = \frac{K\lambda}{\beta\cos(\theta)} \quad (7)$$

$$\boldsymbol{\sigma} = \frac{1}{D^2} \quad (8)$$

3. Results and discussion

3.1. Structural proprieties (X-ray diffraction)

Fig.1 presents the diffractogrammes of the 3 samples of MAPbI3 perovskite deposited on glass substrates with 3 different deposition speeds by the spin-coating technique ((a) 3000, (b)1500 and (c) 400 rpm).

In the 3 samples, the identification of the peaks diffraction shows that the MAPbI3 perovskite crystallizes according to the tetragonal phase and the line (110) exhibit as the preferred growth axis; this orientation is the most preferred for photovoltaic applications [2,13].With 400 rpm the angles located around 2θ =14.01°,19.86°,23.41°,24.38°,28.18°,28.80°,30.54°, 30.96°, 31.62°, 40.23° and 50.17°, with the deposition speed 1500 rpm the perovskite angles located around 2θ =14.33°, 20.30°, 21.18°, 23.64°, 24.31°, 27.53°, 28.68°, 30.84°, 32.06°, 33.51°, 40.73°, 43.56 ° and 59.21° and with 3000 rpm, the perovskite angles located around 2θ =14.28°, 20.17°, 28.56°, 32.29°, 40.58°, 40.81° and 43.42°, this results identical with Ref. [2]. All structural properties of our samples were presented in the table 1, from this table and figure 1(d, e, f), we notice that the deposition speed affect the preferential orientation percentage R(110) which increases with the spinning ,the sample deposited with 3000 rpm give the highest percentage (40,65%), in other hand, the layer thickness decrease, it's may be due to the decrease in the amount of matter with the rotation speed, we notice also that the reflective element of instability (PbI2) was less with the average speed (1500 rpm) where we recorded the highest perovskite percentage (93.71%) and the lowest PbI2 percentage (6.29%), the low percentage of inorganic element indicated the high level of phase purity of the perovskite [27] the sedimentation rate had no effect on other structural properties such as dislocation density and grain size but we can notice that compared to other works which used the ratio (1:1) of (DMF:DMSO), the raise of DMSO ration gave larger grains size [28].

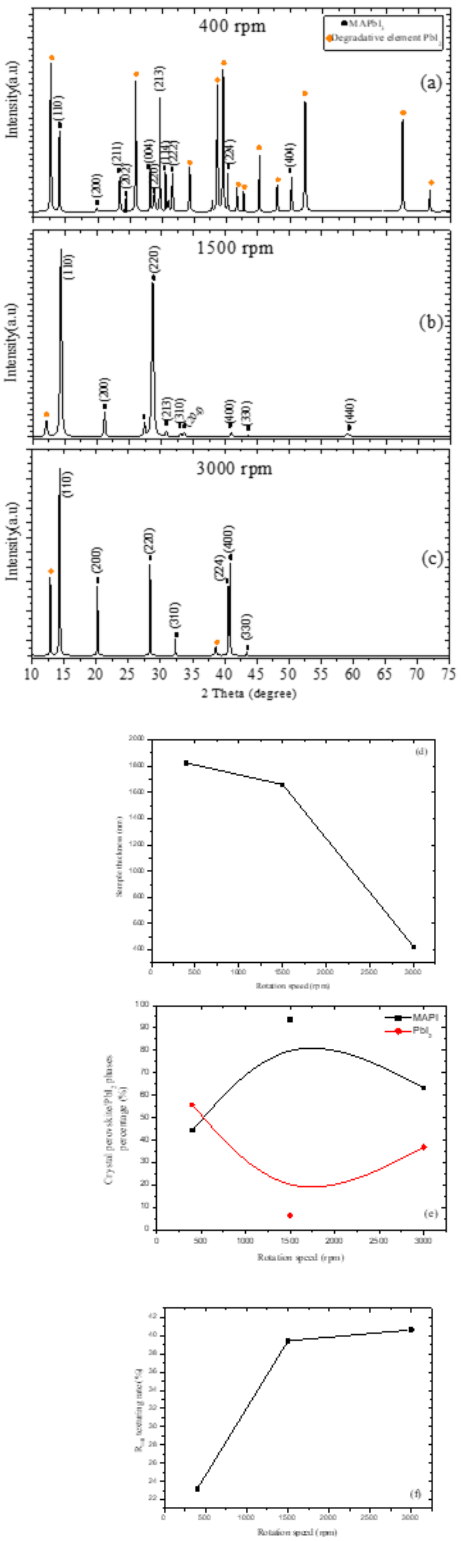

Fig. 1 MAPI3 structural characteristics:(a) diffractogram with 400 rpm deposition speed, (b) with 1500 rpm deposition speed, (c) with 3000 rpm deposition speed, (d) Influence of the deposition speed on the layer thickness, (e) Influence of the deposition speed on the phase percentages (MAPbI3/PbI2) in the crystal and (f) Influence of the deposition rate on the preferential orientation.

Table 1: Structural parameters of MAPI3 samples with different spinning speed.

Spinning speed (rpm)	Preferred orientation R $_{110}$(%)	Layer thickness d ((×10 $^{-9}$m)	$MAPbI_3$ percentage (%)	PbI_2 percentage (%)	Dislocation density δ (×10^{14}lines/m^2)	Grain size D_v (nm)
400	23,19	1807.23	44,29	55,71	0,77	113.60
1500	39,44	843.37	93.71	6.29	1,38	84.96
3000	40,65	421.69	63.23	36.77	0,44	150.53

3.2. Optical proprieties (UV-visible spectroscopy)

For show the change in optical properties, we present the absorbance of our samples with deposition speeds 400, 1500 and 3000 rpm in Fig2 (a), where we notice that the perovskite gives the higher absorbance in the sample deposited with the lowest spinning speed (400 rpm), then, the absorbance begins to decrease with increasing deposition speed in all wavelength range. These results may be due to the amount of material which loss with the rise of rotation speed where the spin coating method considerably changes the density of the material (the solution remaining during the deposition process) [29].

Fig.2 (b, c, d) presents the variation of (αhν)2 versus photon energy ($h\nu$) (Tauc plots) of samples deposited with 400,1500 and 3000 rpm respectively. The intersection point with the ($h\nu$) axis of the linear extrapolation of this curve gives the band gap energy. We notice that the gap energy was not affected by changing the deposition speed. The band gap is determined to be equal to 1.55 eV for all samples with the different speed's deposition. It is noted that these values are in close agreement with the perovskite gap [11].

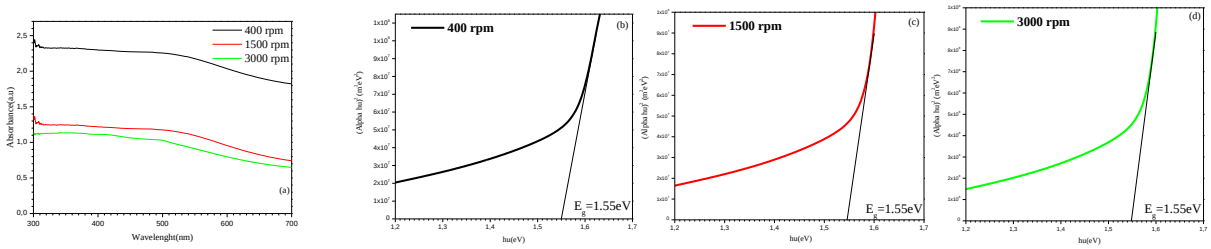

Fig. 2 MAPbI3 optical characteristics:(a) Samples absorbance, (b)Tauc diagram with 400 rpm deposition speed, (c) Tauc diagram with 1500 rpm deposition speed and (d) Tauc diagram with 3000 rpm deposition speed.

4. Conclusion

For a maximum functional diversity in the perovskite MAPbI3 and stable structure we need an optimal deposition speed .The perovskite characteristics are negatively affected such as (low absorbance and the insufficient thickness) if the deposition speed is too high and the very low deposition speed gives high percentage of inorganic element PbI2 (instable structure) and large thickness resulting high dislocation density.

References

[1] T. Miyasaka, impact 2018, 63–65 (2018).

[2] Q.-M. Hong, R.-P. Xu, T.-Y. Jin, J.-X. Tang, et Y.-Q. Li, Organic Electronics 67, 19–25 (2019).

[3] K. Jemli, « Synthése et auto-assemblage de molécules de pérovskite pour la photonique et le marquage », p. 197.

[4] G. Murugadoss, R. Thangamuthu, S. Vijayaraghavan, H. Kanda, et S. Ito, Electrochimica Acta 257, 267–280 (2017).

[5] Rahul et al., Materials Research Bulletin 89, 292–296 (2017).

[6] M. P. Montoya et al., Materials Today: Proceedings 39, 1829–1832 (2021).

[7] I. Mohanty, S. Mangal, S. Jana, et Udai. P. Singh, Adv. Energy Mater. 11, 2002326 (2021).

[8] J. Wei et al., Appl. Phys. Lett. 106, 131904 (2015).

[9] I. Deretzis et al., J. Phys.: Condens. Matter 32, 095501 (2020).

[10] I. S. Zhidkov et al., J. Phys.: Condens. Matter 32, 095501 (2020).

[11] Q.-D. Dao, R. Tsuji, A. Fujii, et M. Ozaki, Organic Electronics 43, 229–234 (2017).

[12] J. Fan, C. Liu, H. Li, C. Zhang, W. Li, et Y. Mai, ChemSusChem 10, 3839–3845 (2017).

[13] S. A. Kahani, E. Maleki, et M. Ranjbar, Journal of Photochemistry and Photobiology A: Chemistry 389, 112218 (2020).

[14] G. S. H. Thien et al., Ceramics International 46, 29041–29051 (2020).

[15] R. Hu et al., Journal of Energy Chemistry 59, 581–588 (2021).

[16] S. C. Ezike, A. B. Alabi, A. N. Ossai, et A. O. Aina, Optical Materials 112, 110753 (2021).

[17] L.-C. Chen, C.-H. Tien, Y.-C. Jhou, et W.-C. Lin, Energies 13, 2438 (2020).

[18] Z. Zhang, Y. Liu, P. Zhang, et Y. Mao, Organic Electronics 88, 106007 (2021).

[19] G. Gordillo, O. G. Torres, M. C. Abella, J. C. Peña, et O. Virguez, Journal of Materials Research and Technology 9, 13759–13769 (2020).

[20] Y.-W. Zhang, P.-P. Cheng, W.-Y. Tan, et Y. Min, Applied Surface Science 537, 147908 (2021).

[21] C. A. López et al., Sci Rep 10, 11228 (2020).

[22] A. A. Ayad, A. Naas, N. Selmi, et O. Meglali, Studies in engineering and exact sciencesTUDIES IN ENGINEERING AND EXACT SCIENCES 5, 306–319 (2024).

[23] Kemerchou et al., J Mater Sci: Mater Electron 32, 3303–3312 (2021).

[24] A. Sami, E. David, et M. Fréchette, in 2010 Annual Report Conference on Electrical Insulation and Dielectic Phenomena 1–4

(IEEE, West Lafayette, IN, 2010).
[25] A. Bouraiou, M. S. Aida, O. Meglali, et N. Attaf, Current Applied Physics 11, 1173–1178 (2011).
[26] S.A.Hassanzadeh-Tabrizi, Journal of Alloys and Compounds 968,171914 (2023).
[27] Z. Liang, S. Zhang, X. Xu, N. Wang, J. Wang, X. Wang, Z. Bi, G. Xu, N. Yuanc, J. Ding, RSC Adv. 5, 60562 (2015).
[28] I. Belaidi, F. Khelfaoui, N. Attaf, A. Azzizi, et M. S. Aida, Phys. Status Solidi A 216, 1900340 (2019).
[29] M. S. Mehde, A. M. Al-Gebori, et A. K. Hantoosh, IOP Conf. Ser.: Mater. Sci. Eng. 757, 012071 (2020).